Dielectric Properties of a Ferroelectric Nematic Material: Quantitative Test of the Polarization-Capacitance Goldstone Mode

Alex Adaka,[1,3] Mojtaba Rajabi,[2] Nilanthi Haputhantrige,[2,3] Samuel Sprunt,[2,3] Oleg D. Lavrentovich,[1,2,3] and Antal Jákli[2,3]

[1]Materials Science Graduate Program, Kent State University, Kent, Ohio 44242, USA
[2]Department of Physics, Kent State University, Kent, Ohio 44242, USA
[3]Advanced Materials and Liquid Crystal Institute, Kent State University, Kent, Ohio 44242, USA

(Received 6 March 2024; accepted 5 June 2024; published 15 July 2024)

The recently discovered ferroelectric nematic (N_F) liquid crystals (LC) have been reported to show an extraordinarily large value of the real part of the dielectric constant ($\varepsilon' > 10^3$) at low frequencies. However, it was argued by Clark *et al.* in Phys. Rev. Res. **6**, 013195 (2024) that what was measured was the capacitance of the insulating layer at LC or electrode surface and not that of the liquid crystal. Here we describe the results of dielectric spectroscopy measurements of an N_F material in cells with variable thickness of the insulating layers. Our measurements quantitatively verify the model by Clark *et al.* Additionally, our measurements in cells with bare conducting indium tin oxide surface provide a crude estimate of $\varepsilon_\perp \sim 10^2$ in the N_F phase.

DOI: 10.1103/PhysRevLett.133.038101

The recently discovered ferroelectric nematic (N_F) liquid crystas [1–5] exhibit large ferroelectric polarization P in the range of $(4\text{–}7) \times 10^{-2}$ C/m^2 that is unprecedented in liquid crystals, and are also reported to show an extraordinarily large real part of the dielectric permittivity ($\varepsilon' > 10^3$) at low frequencies [3,4,6–9]. Recently, Clark *et al.* [10,11] have argued that the measured large dielectric constant of N_F is an artifact and what has been measured is the capacitance of the nonferroelectric interfacial insulating layer at the N_F/electrode surface and not that of the liquid crystal. This is due to the block reorientation of the large polarization **P** of N_F, which renders the liquid crystal layer conductive, enabling the insulating interfacial layers to charge up. This mechanism leads to a polarization-capacitance Goldstone (PCG) mode with the apparent real $\varepsilon'_A(\omega)$ and imaginary $\varepsilon''_A(\omega)$ components of the dielectric spectra [10,11],

$$\varepsilon'_A(\omega) = \varepsilon_A(0)\frac{1}{1+(\omega\tau_o)^2} \text{ and } \varepsilon''_A(\omega) = \varepsilon_A(0)\frac{\omega\tau_o}{1+(\omega\tau_o)^2}. \quad (1)$$

Here $\varepsilon_A(0) = \varepsilon_I d/d_I$, where ε_I and d_I are the dielectric constant and thickness of the insulating layer, respectively, and d is the thickness of the liquid crystal film. Furthermore, the characteristic relaxation time in the N_F cell is $\tau_o = (\varrho_{LC}\varepsilon_o\varepsilon_I d/d_I) = R_{LC}C_I$, where $\varrho_{LC} = \gamma/P^2$ is the effective resistivity of the LC, γ is the rotational viscosity, and C_I is the capacitance of the insulating layer. This results in an approximation for the relaxation frequency $f_o^{N_F}$ as

$$f_o^{N_F} = \frac{1}{2\pi\tau_o} = \frac{P^2}{2\pi\gamma\varepsilon_o\varepsilon_I}\cdot\frac{d_I}{d}. \quad (2)$$

More recently, Vaupotič *et al.* [12] studied homologues series of RM734 [1,4,13] sandwiched between conducting layers. The dielectric constant in the N_F phase was found to exceed 10^4, in accordance with previous measurements [3,4,6–8]. To interpret the results, Vaupotič *et al.* [12] proposed a continuous phenomenological model (CPM) in which the dielectric response is dominated by flexoelectricity, being relevant only at a very weak surface anchoring. In this condition the relaxation frequency f_o becomes thickness dependent, $f_o \propto \left[\alpha + (\beta/d) + (c/d^2)\right]$, where α, β, and c are phenomenological constants.

Experimentally Erkoreka *et al.* found that the measured dielectric strength (relaxation frequency) is proportional (inversely proportional) to the film thickness at low frequency, and independent of film thickness at high frequency [14,15]. This behavior is in qualitative agreement with the PCG [11], the CPM [12] (for $\alpha = c = 0$), and also with the electrode polarization (EP) mode known for conductive samples with electric double layers near the substrates [16]. In fact, the PCG model can be considered a particular realization of the EP mode, as the ferroelectric nematic can be considered as the "conductive sample" and C_I relates to "electric double layers" near the substrates.

Finally, very recently Matko *et al.* [17] analyzed impedance measurements carried out on several RM734 cells of different thicknesses d and based on their simulation results they concluded "that the relative permittivity of the

ferroelectric nematics is indeed huge, and it is even higher than the apparent measured values".

In this Letter we describe the results of dielectric spectroscopy measurements of an N_F material in cells with a controlled thickness of the insulating alignment layer (as was done for SmC* materials by Coleman *et al.* [18]) and cells with bare conducting indium tin oxide (ITO) surface. We find excellent quantitative agreement with Eq. (1) and good agreement with Eq. (2) derived by Clark *et al.* using the PCG model [11].

We study a liquid crystal UUZU-4-N provided by Merck [19]. On cooling, the material exhibits three nematic phases labeled as N, N_X, and N_F with phase sequence in °C: $\mathrm{I} - 94.1 - N - 92.4 - N_X - 86.2 - N_F - 60 - \mathrm{Cr}$. The molecular structure of UUZU-4-N together with the temperature dependence of the ferroelectric polarization and the switching voltages are shown in Fig. S1 of the Supplemental Material [20]. The calculated [B3LYP/6-31G(d)] dipole moment of a single molecule is $\mu \approx 11.9$ D [19]. Results of the switching time measurements are described and shown in Fig. S2 in the Supplemental Material [20] which includes [21–23]. Details of sample preparation, including the technique of preparing insulating PI2555 polyimide insulating layers with controlled thicknesses $d_I/2$, and the dielectric measurement technique are also described in the Supplemental Material [20].

The frequency dependences of the imaginary part of the dielectric constant ε'' at several selected temperatures for four cells with different insulating layer thickness d_I values are shown in Figs. 1(a)–1(d).

In the N_F phase (below 86 °C) the apparent dielectric spectra $\varepsilon_A(f)$ show a peak at frequencies corresponding to the relaxation frequencies $f_o^{N_F}$. Assuming Debye relaxation, the maxima correspond to half of the susceptibility $(\chi/2) = \{[\varepsilon(0) - \varepsilon(\infty)]/2\}$. It is found that $f_o^{N_F}$ increases from ~15 to 150 kHz, and χ decreases from ~360 to ~100 when d_I increases from ~90 nm to ~334 nm.

In the N phase the relaxation frequencies vary from a few hundred Hz to a few kHz, i.e., an order of magnitude smaller than in the N_F phase, while their d_I/d dependences show similar trends to that in the N_F phase. In the N_X phase

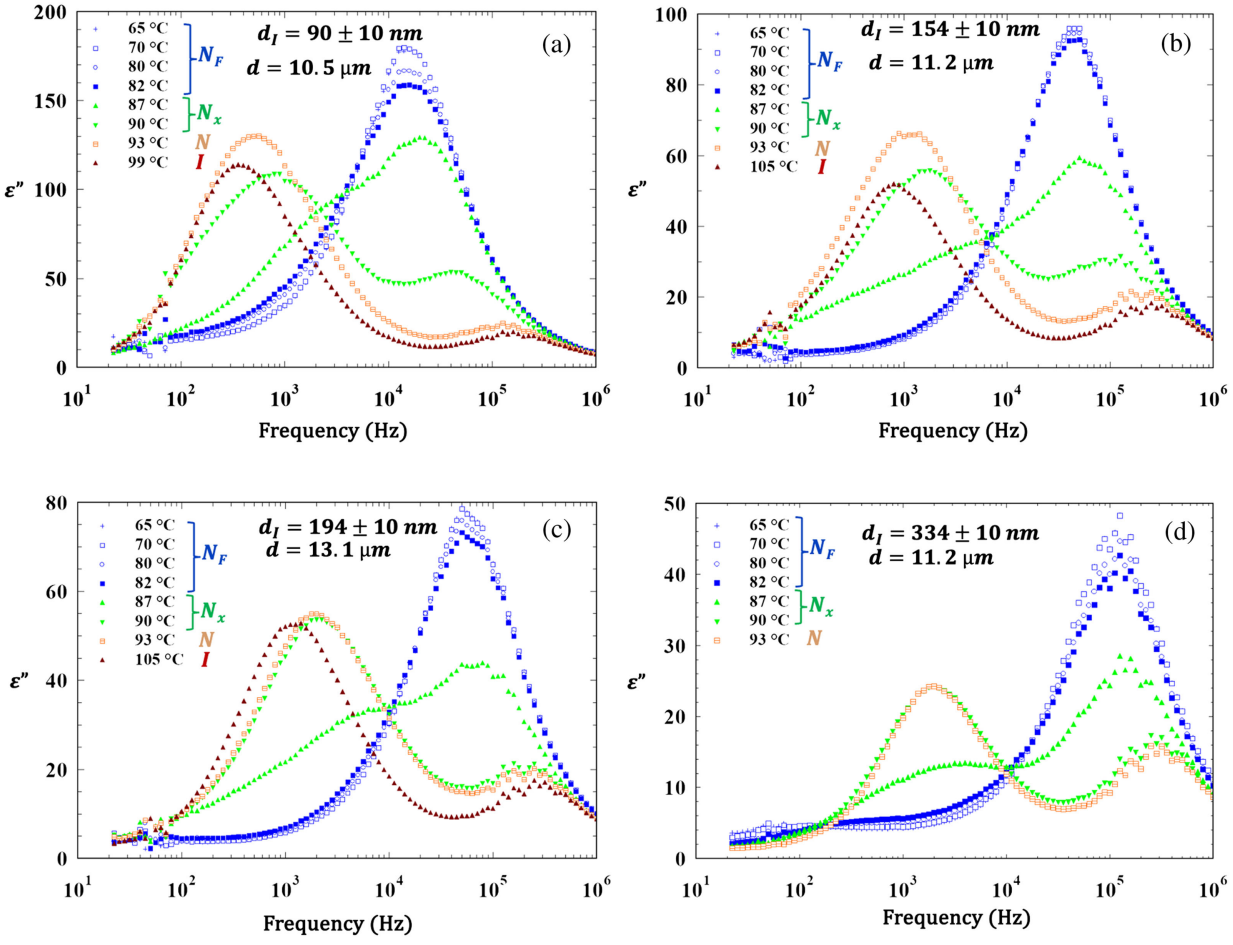

FIG. 1. Frequency dependences of the imaginary part of the dielectric constant ε'' at several selected temperatures for (a) $d \approx 10.5$ μm and $d_I \approx 90$ nm; (b) $d \approx 11.2$ μm and $d_I \approx 154$ nm; (c) $d \approx 13.1$ μm and $d_I \approx 194$ nm; (d) $d \approx 11.2$ μm and $d_I \approx 334$ nm film and alignment layer thicknesses.

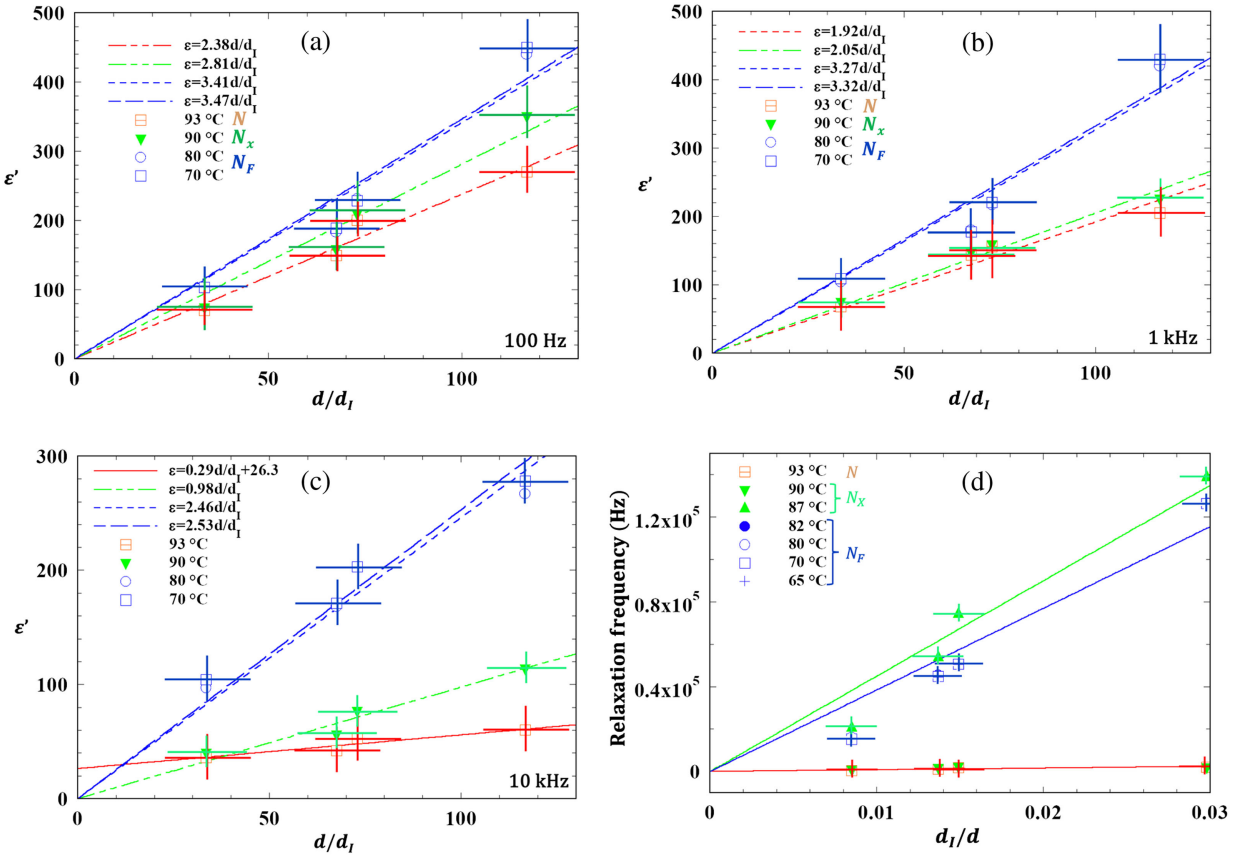

FIG. 2. The measured ε' as a function of d/d_I at 100 Hz (a), 1 kHz (b), and at 10 kHz (c) at various temperatures. (d) The relaxation frequency as a function of d_I/d at various temperatures. Lines represent the best fits with slopes 8×10^4, 4.5×10^6, and 3.85×10^6 Hz in the N, N_X, and N_F phases, respectively.

there are two peaks; one in the kHz, and one in the 10–100 kHz range. The closer to the N_F phase, the larger (smaller) is the maxima of the higher (lower) frequency peaks, indicating that the N_X phase has coexisting N_F and N domains. Optically this coexistence cannot be seen, which indicates that the size of these domains is below 1 μm. In the I, N_X, and N phases we see an additional peak above 300 kHz.

To verify Eq. (1), in Figs. 2(a)–2(c) we plot the measured ε' values versus d/d_I at 0.1, 1, and at 10 kHz. 100 Hz is well below the relaxation frequencies, thus ε' is approximately equal to $\varepsilon'_A(0)$; 1 kHz is close to the relaxation frequencies found in the N_X and N phases; and 10 kHz is below the relaxation frequencies found in the N_F phase, but above the relaxation frequencies found in the N_X and N phases. According to Eq. (1), the slope of $\varepsilon'_A(d/d_I)$ should give $\{\varepsilon_I/[1+(\omega\tau_o)^2]\}$. It can be seen in Figs. 2(a)–2(c) that within the measurement error, the d/d_I dependence of ε'_A is linear at all temperatures. Notably, at 100 Hz, in the N_F phase the slopes of the best fits are nearly constant (~3.5), corresponding to the dielectric constant of the polyimide PI2555 [24]. At 1 kHz [see Fig. 2(b)] and at 10 kHz [see Fig. 2(c)] the slopes in the N_F phase are still almost temperature independent, but they have smaller values: ~3.3 for 1 kHz and ~2.5 at 10 kHz, a decrease caused by the factor $\{1/[1+(\omega\tau_o)^2]\}$. These observations quantitatively agree with Eq. (1), and thus completely support the model by Clark *et al.* [11].

Although the PCG model is not applicable to the N phase, we find a similar d/d_I dependence with a much smaller slope than in the N_F phase. This behavior is likely related to the large conductivity with electric double layer near the substrate (EP mode) [16]. The decrease of the slopes in the N_X phase is in between those in the N_F and N phases, which is understandable, taking into account that N_X is characterized both by the low and high frequency relaxations.

The d_I/d dependence of the measured relaxation frequencies at several temperatures in the N_F, N_X, and N phases are shown in Fig. 2(d). The best fits assuming $f_o \propto (d_I/d)$ corresponding to Eq. (2) have almost the same slopes [in the range of $(3.8-4.4)\times 10^6$ s^{-1}] in the N_F phase, ~4.5×10^6 s^{-1} the N_X phase, and 8×10^4 s^{-1} in the N phase. In the N_F phase Eq. (2) gives $\gamma \approx \{(6\times10^{-2})^2/[2\pi\cdot(3.8\text{–}4.4)\times10^6\cdot3.1\times10^{-11}]\} \sim (4.2\text{–}4.9)$ Pa·s. These values are several times larger than what we obtained from the switching time measurements (see Supplemental

Material [20] and Fig. S2). This difference is not surprising, since the dielectric experiments in sandwich cell mainly test splay deformation, while the in-plane field-induced, full polarization switching involves twist.

In the N and I phases the polarization is zero, and Eq. (2) is not applicable. We propose that the measured large dielectric constant below the kHz relaxation frequency range is due to the high conductivity of UUZU-4-N in the isotropic phase. Following the argument of Clark *et al.* [11], $R_{LC} = (d/A\sigma)$, so the relaxation time is $\tau_o = R_{LC} \cdot C_I = (\varepsilon_o \varepsilon_I/\sigma) \cdot (d/d_I)$. Accordingly,

$$f_o^N = \frac{1}{2\pi\tau_o} = \frac{\sigma}{2\pi\varepsilon_o\varepsilon_I} \cdot \frac{d_I}{d}. \tag{3}$$

With the fit value of 8×10^4 s^{-1} at 93 °C[see Fig. 2(d)], Eq. (3) provides $\sigma \sim 1.5 \times 10^{-5}$ $1/(\Omega\text{m})$. We note that it will slightly modify Eq. (2) as $f_o^{N_F} = [(P^2 + \gamma\sigma)/(\gamma\varepsilon_o \cdot \varepsilon_I)] \cdot (d_I/d)$. However, $\gamma\sigma \ll P^2$, i.e., the effect of electric conductivity can be neglected in the N_F phase.

Importantly, ε_A'' measured at high frequencies for different cells show similar values regardless of the values of d and d_I, Fig. 3. This result confirms Eq. (1) of the PCG model, which for large frequencies, $\omega\tau_o \gg 1$, simplifies to $\varepsilon_A''(\omega) = \varepsilon_I(d/\omega\tau_o d_I)$. Since the relaxation time is $\tau_o = (\varrho_{LC}\varepsilon_o\varepsilon_I d/d_I)$, one finds

$$\varepsilon_A''\left(f \gg \frac{2\pi}{\tau_o}\right) \approx \frac{1}{2\pi f \varrho_{LC}\varepsilon_o}, \tag{4}$$

which does not depend on d nor on d_I. To illustrate the overlap, Fig. 3 shows together the $\varepsilon_A''(f)$ curves measured at different temperatures in the N_F phase and for different d_I. We also plotted the fits for $d_I = 90$ *and* 154 nm. The best fits yield $\varrho_{LC}\varepsilon_o = (2.2\text{–}2.76) \times 10^{-8}$ s, which corresponds

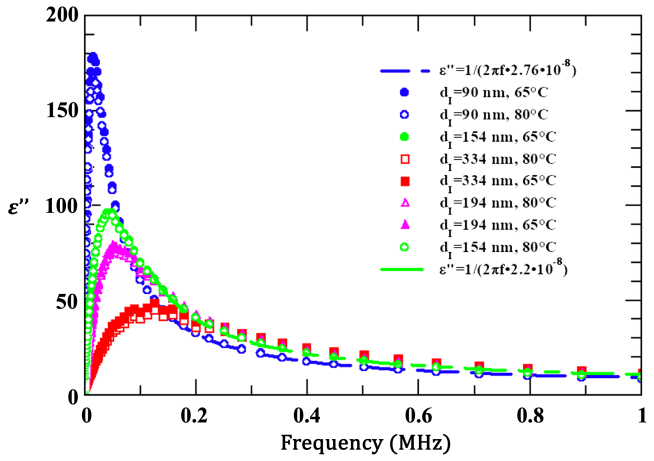

FIG. 3. The measured $\varepsilon_A''(f)$ curves in linear scale in the N_F phase at 65 °C and 80 °C for all insulating layer thicknesses. Dashed blue and green lines correspond to fits to Eq. (4) for $d_I = 90$ and 154 nm, respectively.

to resistivity $\varrho_{LC} \sim (2.5\text{–}3.1) \times 10^3$ Ωm. Assuming $\varrho_{LC} \sim \gamma/P^2$, one gets $\gamma \sim 5\text{–}10$ Pa · s, which is comparable to the viscosity values obtained from the d_I/d dependence of the relaxation frequencies, as shown in Fig. 2(d).

We have carried out additional measurements using bare ITO coated substrates. The frequency dependent spectra of ε' and ε'' at selected temperatures are shown in Figs. 4(a) and 4(b) for $d = 10.9$ μm and in Figs. 4(c) and 4(d) for $d = 17.2$ μm films, respectively. One can see that in the isotropic and nematic phases ε'' decreases monotonously without showing any peak above 20 Hz. According to Eq. (3), the decreasing frequency of the peak position should be due to the effectively much smaller insulating layer thickness on bare ITO substrates. For the same reason, in the N_F phase the relaxation frequency on bare ITO substrates is also about 1 order of magnitude smaller than in the PI2555 coated cells. Importantly, the measured low frequency dielectric constants now approaching $\varepsilon_A(0) \sim 8 \times 10^3$ in the $d = 10.9$ μm sample and $\varepsilon_A(0) \sim 1.7 \times 10^4$ for $d = 17.2$ μm sample, similar to those reported by others in samples with gold electrodes [3,4,6–9]. As the alignment even in bare ITO cells is close to planar, such as in the PI2555 coated cells, we conclude that the large difference is due to the much thinner insulating layer $d_I = [\varepsilon_I/\varepsilon_A(0)]d$, which assuming that ε_I on the bare ITO is similar to dielectric polymers, provides $d_I \approx 4.8$ and ≈3.5 nm for the 10.9 and 17.2 μm cells, respectively.

This indicates that the thickness of the insulating layer on each substrate ξ_I is $1.8 < \xi_I < 2.4$ nm, which is comparable to the molecular length. We note here that Clark *et al.* [11] state that even at conducting substrates (such as the bare ITO), there should be a layer of thickness

$$\xi_I = \sqrt{\frac{\varepsilon_o\varepsilon_{LC}K}{P^2}}, \tag{5}$$

where the polarization space charge is expelled and should be considered as non-ferroelectric insulating layer. In the above expression K is an effective Frank elastic constant and ε_{LC} is the bare N_F dielectric constant. Using $K \sim 10$ pN, we can estimate that $\varepsilon_{LC} \approx (\xi_I^2 P^2/K\varepsilon_o) \sim 120$ for the 10.9 μm cell and $\varepsilon_{LC} \sim 230$ for 17.2 μm cell. The difference between the calculated apparent dielectric constants can be due to slight alignment differences, or simply due to the fact that the apparent thickness of the insulating layers might be different from ξ_I because of oxidation or any dirt. For this reason, the above estimated ε_{LC} values are likely larger than the actual values.

Using $d_I \approx 4.8$ and ≈3.5 nm for the 10.9 and the 17.2 μm cells, from Eq. (2) we can also estimate the rotational viscosity values to be $\gamma \approx 4.4$ and 4.2 Pa s, respectively. These values are similar that those we obtained for the PI coated cells, thus indicating that the alignment on the bare ITO coated cells is also very close to planar and represents rotations involving mainly splay.

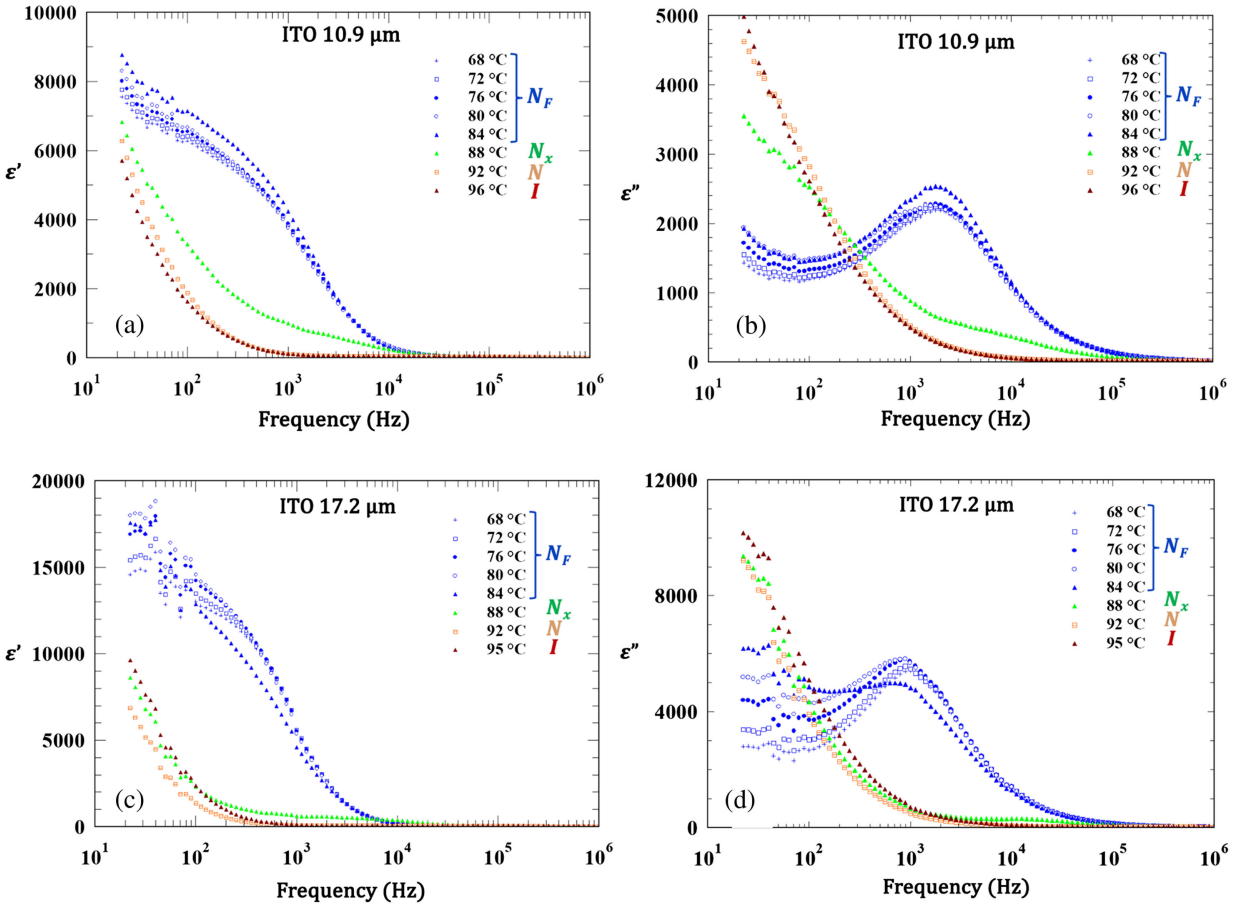

FIG. 4. $\varepsilon'(f)$ and $\varepsilon''(f)$ of bare ITO coated sandwich cells at various temperatures. (a) and (b) $\varepsilon'(f)$ and $\varepsilon''(f)$ of 10.9 μm film, respectively; (c) and (d) $\varepsilon'(f)$ and $\varepsilon''(f)$ of 17.2 μm film, respectively.

To summarize, detailed analysis of our measurements on UUZU-4-N in the frame of the polarization-capacitance Goldstone model of Clark *et al.* [11] provided quantitative agreement in terms of the measured dielectric constant as a function of d/d_I, verifying that the measured dielectric constant is determined by the capacitance of the insulating layer and does not represent the dielectric permittivity of the ferroelectric nematic. The often reported extraordinary high values of the apparent dielectric permittivity of the N_F phase are the result of "block polarization reorientation" which screens the applied electric field within the N_F cell. The applied voltage acts only at the insulating layers such as polyimide coatings. The apparent dielectric permittivity $\varepsilon_A(0) = \varepsilon_I d/d_I$ is then a characteristic of the insulating layers. A large d/d_I value produces an apparent $\varepsilon_A(0)$ on the order of 10^4. Comparing the measured d_I/d dependence of the relaxation frequency with Eq. (2) further confirms the PCG model. We could then use our results on films with bare ITO substrates to estimate the thickness of dielectric layer adjacent to the ITO substrate to be $(d_I/2) \sim 2$ nm. With this, using again the PCG model [11], we estimate the dielectric constant when the polarization is perpendicular to the electric field, to be $\varepsilon_\perp \sim 10^2$.

This work was financially supported by U.S. National Science Foundation Grant No. DMR-2210083 (A. J. and S. S.), DMR-2215191 (O. D. L., digital holographic microscopy studies), and ECCS-2122399 (O. D. L., analysis of switching). The material UUZU-4-N was provided by Merck Electronics KGaA, Darmstadt, Germany.

[1] R. J. Mandle, S. J. Cowling, and J. W. Goodby, A nematic to nematic transformation exhibited by a rod-like liquid crystal, Phys. Chem. Chem. Phys. **19**, 11429 (2017).
[2] H. Nishikawa and F. Araoka, A new class of chiral nematic phase with helical polar order, Adv. Mater. **33**, 1 (2021).
[3] N. Sebastián, M. Čopič, and A. Mertelj, Ferroelectric nematic liquid crystalline phases, Phys. Rev. E **106**, 021001 (2022).
[4] N. Sebastián, L. Cmok, R. J. Mandle, M. R. De La Fuente, I. Drevenšek Olenik, M. Čopič, and A. Mertelj, Ferroelectric-ferroelastic phase transition in a nematic liquid crystal, Phys. Rev. Lett. **124**, 037801 (2020).
[5] X. Chen *et al.*, First-principles experimental demonstration of ferroelectricity in a thermotropic nematic liquid crystal:

Polar domains and striking electro-optics, Proc. Natl. Acad. Sci. U.S.A. **117**, 14021 (2020).
[6] R. J. Mandle, N. Sebastián, J. Martinez-Perdiguero, and A. Mertelj, On the molecular origins of the ferroelectric splay nematic phase, Nat. Commun. **12**, 4962 (2021).
[7] R. Saha, P. Nepal, C. Feng, M. S. Hossain, M. Fukuto, R. Li, J. T. Gleeson, S. Sprunt, R. J. Twieg, and A. Jákli, Multiple ferroelectric nematic phases of a highly polar liquid crystal compound, Liq. Cryst. **49**, 1784 (2022).
[8] H. Nishikawa, K. Shiroshita, H. Higuchi, Y. Okumura, Y. Haseba, S. I. Yamamoto, K. Sago, and H. Kikuchi, A fluid liquid-crystal material with highly polar order, Adv. Mater. **29**, 1702354 (2017).
[9] N. Yadav, Y. P. Panarin, J. K. Vij, W. Jiang, and G. H. Mehl, Polar nature of the ferroelectric nematic studied by dielectric spectroscopy, arXiv:2203.04944.
[10] N. A. Clark, X. Chen, J. E. Maclennan, and M. A. Glaser, Dielectric spectroscopy of ferroelectric nematic liquid crystals: Measuring the capacitance of insulating interfacial layers, arXiv:2208.09784.
[11] N. A. Clark, X. Chen, J. E. MacLennan, and M. A. Glaser, Dielectric spectroscopy of ferroelectric nematic liquid crystals: Measuring the capacitance of insulating interfacial layers, Phys. Rev. Res. **6**, 013195 (2024).
[12] N. Vaupotič, D. Pociecha, P. Rybak, J. Matraszek, M. Čepič, J. M. Wolska, and E. Górecka, Dielectric response of a ferroelectric nematic liquid crystalline phase in thin cells, Liq. Cryst. **50**, 584 (2023).
[13] A. Mertelj, L. Cmok, N. Sebastián, R. J. Mandle, R. R. Parker, A. C. Whitwood, J. W. Goodby, and M. Čopič, Splay nematic phase, Phys. Rev. X **8**, 041025 (2018).
[14] A. Erkoreka, J. Martinez-Perdiguero, R. J. Mandle, A. Mertelj, and N. Sebastián, Dielectric spectroscopy of a ferroelectric nematic liquid crystal and the effect of the sample thickness, J. Mol. Liq. **387**, 122566 (2023).
[15] A. Erkoreka, A. Mertelj, M. Huang, S. Aya, N. Sebastián, and J. Martinez-Perdiguero, Collective and non-collective molecular dynamics in a ferroelectric nematic liquid crystal studied by broadband dielectric spectroscopy, J. Chem. Phys. **159**, 184502 (2023).
[16] F. Kremer and A. Schönhals, *Broadband Dielectric Spectroscopy* (Springer Berlin Heidelberg, Berlin, Heidelberg, 2003).
[17] V. Matko, E. Górecka, D. Pociecha, J. Matraszek, and N. Vaupotič, Do ferroelectric nematic liquid crystals really have a huge dielectric permittivity?, arXiv:2401.16084.
[18] D. Coleman, D. Mueller, N. A. Clark, J. E. Maclennan, R. F. Shao, S. Bardon, and D. M. Walba, Control of molecular orientation in electrostatically stabilized ferroelectric liquid crystals, Phys. Rev. Lett. **91**, 175505 (2003).
[19] A. Manabe, M. Bremer, M. Kraska, and M. Klasen-Memmer, Polar Liquid Crystals for Highly Ordered Nematics, IDW (2021), 10.36463/idw.2021.0050.
[20] See Supplemental Material at http://link.aps.org/supplemental/10.1103/PhysRevLett.133.038101 for polarization, threshold voltage and switching time measurements, details of sample preparation and technical details of dielectric spectroscopy.
[21] X. Chen *et al.*, The smectic ZA phase: Antiferroelectric smectic order as a prelude to the ferroelectric nematic, Proc. Natl. Acad. Sci. U.S.A. **120**, e2217150120 (2023).
[22] C. Feng, R. Saha, E. Korblova, D. Walba, S. N. Sprunt, and A. Jákli, Electrically tunable reflection color of chiral ferroelectric nematic liquid crystals, Adv. Opt. Mater. **9**, 2101230 (2021).
[23] A. Jákli and A. Saupe, *One- and Two- Dimensional Fluids: Properties of Smectic, Lamellar and Columnar Liquid Crystals*, 1st ed. (Taylor and Francis, Boca Raton, 2006).
[24] A. W. Lin, Evaluation of polyimides as dielectric materials for multichip packages with multilevel interconnection structure, IEEE Trans. Components, Hybrids, Manuf. Technol. **13**, 207 (1990).